RSC Advances

PAPER

Check for updates

Catalytic synthesis of chloroacetates with thermoregulated ionic liquids based on vanadium-substituted polyoxometalate

Jingsen Yan,[a] Zeqing Wang,[a] Yongsheng E,[a] Fengwei He,[a] Danfeng Zhang[a] and Qingyin Wu ⓘ *[ab]

A series of polyoxometalate-based ionic liquid (POM-IL) catalysts with functional sulfonic acid groups, $[TEAPS]_{3+n}PW_{12-n}V_nO_{40}$ (n = 1, 2, 3) were synthesized and characterized by nuclear magnetic resonance spectroscopy (NMR), Fourier transform infrared spectrophotometry (FT-IR), UV-Vis spectrophotometry (UV), potentiometric titration and thermogravimetry-differential scanning calorimetry (TG-DSC). The catalytic ability and reusability of the POM-IL catalysts were evaluated on esterification of chloroacetic acid and n-amyl alcohol. The optimum reaction conditions, 0.2 g of the catalyst amount, 10 mL of water carrier, 140 °C of reaction temperature, and 1.2/1 of the molar ratio of alcohol/acid, were obtained by an orthogonal test. $[TEAPS]_5PW_{10}V_2O_{40}$ was found to be the best active catalyst with an esterification rate of 98.75% and could be reused five times without significant decrease in activity. The ionic liquid acted as a temperature-responsive catalyst, forming a homogeneous mixture with the reactants at reaction temperature, and could be precipitated and separated from products when the reaction ends at ambient temperature. Therefore, an environmentally friendly and highly efficient approach for the synthesis of chloroacetates is provided.

1. Introduction

Chloroacetates are important organic synthesis intermediates in medicine, pesticides, plasticizers, and preparation of the esters is mostly achieved through acid-catalyzed reaction processes with mineral acids, such as H_2SO_4, HCl, H_3PO_4.[1–3] However, these acids as homogenous catalysts are hardly separated and reused. Furthermore, these acids are highly corrosive and need to be neutralized at the end of the esterification reaction.[4–6] Thus, various heterogeneous catalysts, such as polyoxometalates (POM), acidic resins, solid superacids have been explored as alternatives.[7–9] However, these catalysts also have some disadvantages such as easy deactivation and high mass transfer resistance, which limit their application.

In response to both the advantages and disadvantages of homogeneous and heterogeneous catalysts, phase-transfer catalysts and temperature regulated catalysts have attracted much attention.[10,11] Among them ionic liquids (ILs) have been regarded as green reaction media or promise catalyst owing to their excellent thermal stability, outstanding solubility, negligible volatility, diversified structure and physiochemical properties.[12–14] Cations and anions of ILs can be fashioned to bind specific functional group for specific chemical applications.[15,16]

Cole *et al.* firstly synthesized Brønsted acidic ILs that bear an alkyl sulfonic acid group in imidazolium cations or triphenylphosphine cations.[17] These Brønsted acidic ionic liquids exhibited temperature-controlled liquid–solid separation as solvent/catalysts for Fischer esterification and the pinacol rearrangement. Then, there were many articles on the functionalized ILs used in different esterification, the esterification system is homogeneous at reaction temperature and heterogeneous at the end of reaction.[18–20] However the ionic liquid catalysts is also not an excellent candidate owing to high content of ionic liquid needed in the reaction and relatively long reaction time.

In order to resolve this problem, the design and synthesis of polyoxometalate-based ionic liquid catalysts (POM-ILs) have been applied in esterification reaction.[21–24] However, the regular anion in POM-ILs is binary polyoxometalate rather than ternary, only a few reports focus on ternary polyoxometalate. In fact, ternary polyoxometalates usually show more perfect properties than binary ones such as reversible thermal response and electrochemical performance.[25–28] Herein, a series of novel polyoxometalate ionic liquid catalysts were prepared by using an organic ammonium, 1-(3-sulfonic group) grafted triethylamine (TEAPS) and vanadium-substituted ternary heteropolyacids. The catalysts have good activity and reusability in esterification system owing to their acidity and thermoregulated property. Their structures, activities in esterification, reversible thermal

[a]*School of Biomedical & Chemical Engineering, Liaoning Institute of Science and Technology, Benxi 117004, Liaoning, P. R. China. E-mail: qywu@zju.edu.cn*

[b]*Department of Chemistry, Zhejiang University, Hangzhou, 310027, P. R. China*

responsive properties and reaction mechanism are also investigated.

2. Experimental section

2.1 Instrumentation and reagents

^{1}H NMR and ^{13}C NMR spectra were recorded on a Bruker AVANCE 500 MHz spectrometer in D_2O. Solid-state ^{31}P MAS NMR spectra was carried out on a Varian 400 InfinityPlus spectrometer at relaxation delay of 4 s. Infrared spectra was measured by Beijing Beifen-Ruili WQF-510A FT/IR spectrometer during the wavenumber range 400–4000 cm^{-1} using KBr pellet. UV absorption spectra was monitored by a Beijing Persee Spectrord TU-1901 UV-Vis spectrophotometer during scanning range 190–400 nm. X-ray powder diffraction analysis was conducted on a BRUKER D8 ADVANCE X-ray diffractometer using a Cu tube operated at 40 kV and 40 mA in the range of $2\theta = 4$–$40°$ at a rate of 0.02° s^{-1}. The thermal stability of samples was investigated on a SHIMADZU thermal analyser in the range of 25–550 °C at a rate of 10 °C min^{-1}. The reaction products were measured by Agilent 1200 high performance liquid chromatography (HPLC). Melting point of samples was measured using WRS-1B digital microscopic melting point apparatus. The acidity of samples was determined using potentiometric titration. For the potentiometric titration, 0.1 g of POM-ILs solid was dissolved in menthol (25 mL). The solution was titrated with 0.01 mol L^{-1} solution of n-butylamine in acetonitrile. The potential variation was measured by Shanghai Leici pHS-2F digital acidity meter using pH composite electrode.

All the chemicals were of analytical grade and used without further purification.

2.2 Synthesis of the POM-ILs catalysts

Synthesis procedure of the POM-ILs was expressed in the following schematic Fig. 1. TEAPS was synthesized according to the literature,[21] and the detailed procedure was as follows: 1,3-propane sultone (0.066 mol) and triethylamine (0.066 mol) were dissolved in acetone(13 mL). Then they were mixed and stirred at 50 °C for 12 h. A white precipitate (TEAPS) was filtered, washed with acetone three times, and dried at 60 °C in a vacuum. A series of polyoxometalate (POM), $H_4[PW_{11}VO_{40}]$, $H_5[PW_{10}V_2O_{40}]$, $H_6[PW_9V_3O_{40}]$ and the POM-ILs were synthesized according to the literatures.[29–32] The synthesis method of POM-ILs catalysts are as follows: the pre-synthesized TEAPS and POM, $H_4[PW_{11}VO_{40}]$, $H_5[PW_{10}V_2O_{40}]$, $H_6[PW_9V_3O_{40}]$ were taken in 4 : 1, 5 : 1 and 6 : 1 molar ratio to give one mole of $[TEAPS]_4PW_{11}VO_{40}$, $[TEAPS]_5PW_{10}V_2O_{40}$, and $[TEAPS]_6PW_9V_3O_{40}$. TEAPS was added into an aqueous solution of various POM, respectively. The mixture was stirred for 12 h at room

temperature. Water was firstly evaporated in a water bath at 50 °C and then removed under vacuum at 60 °C to give the final products. The obtained $[TEAPS]_4PW_{11}VO_{40}$, $[TEAPS]_5PW_{10}V_2O_{40}$ and $[TEAPS]_6PW_9V_3O_{40}$ were pale yellow powder, yellow quasi solid and brown gel-type solid, and their melting points were determined to be 145.0 °C, 105.4 °C and 88.1 °C, respectively.

2.3 Procedure for esterification reactions

The typical esterification reaction process was as follows: chloroacetic acid (0.16 mmol), 1-pentanol (0.192 mmol), POM-ILs catalysts (0.5 g) and benzene (10 mL) were added into a three-necked flask with a water segregator. The reaction was refluxed at 140 °C with stirring until the water separated in the water segregator no longer increases. The products were analysed by HPLC with external standard method. The determination conditions were as follows: Agilent ZORBAX XDB-C18 column (4.6 × 150 mm), UV absorbance detector at 213 nm, and the mobile phase was ethanol and water (65 : 35, v/v), flow rate at 1.0 mL min^{-1} and column temperature at 20 °C. Esterification rate was calculated by conversion of chloroacetic as follows:

$$Y = \frac{(C_0 - C_R)}{C_0} \times 100$$

wherein C_0 was initial content of chloroacetic acid and C_R was chloroacetic acid content at the end of reaction.

3. Results and discussion

3.1 NMR analysis

Fig. 2 shows the ^{1}H NMR spectrum (Fig. 2a), ^{13}C NMR (Fig. 2b) and ^{31}P MAS NMR of $[TEAPS]_5PW_{10}V_2O_{40}$. The ^{1}H NMR chemical shift values (ppm) are: δ 1.33 (t, 9H), 2.15 (m, 2H), 2.98 (t, 2H), 3.17 (t, 2H), and 3.36 (m, 6H), corresponding to the structural formula ($[(C_2H_5)_3N(CH_2)_3SO_3H]PW_{10}V_2O_{40}$). Peaks at 1.33 ppm and 3.36 ppm correspond to methyl and methylene in ethyl group, respectively. Peaks at 2.15 ppm, 2.98 ppm and 3.17 ppm correspond to three methylene linking to N and S atoms.[21] The ^{13}C NMR chemical shift values (ppm) for $[TEAPS]_5PW_{10}V_2O_{40}$ are: δ 9.61, δ 20.16, δ 50.08, δ 55.77, and δ 57.75, representing carbon atoms in five different chemical environments, respectively. For the solid ^{31}P MAS NMR spectra (Fig. 2c), the sharp resonance at −15.4 ppm was assigned to the chemical shift of phosphorus, and the peak value is a little more negative compared to the corresponding signal from HPW($\delta_p = $ −15.0 ppm).[33] It may be a result of the interaction between the Keggin tungstophosphate anion and the V^{5+} ion after the synthesis of $[TEAPS]_5PW_{10}V_2O_{40}$. The results indicated that the heteropoly acid and TEAPS were successfully assembled.

3.2 FTIR and UV analysis

Fig. 3 shows FT-IR spectra of $H_5[PW_{10}V_2O_{40}]$, fresh $[TEAPS]_5PW_{10}V_2O_{40}$ and recycled $[TEAPS]_5PW_{10}V_2O_{40}$. The wavenumber of major bands of the compounds are given in the Table 1. As seen from Fig. 3 and Table 1, there were four characteristic vibrational bands which were assigned to $\nu_{as}(P–O_a)$, $\nu_{as}(M=O_d)$, $\nu_{as}(M–O_b–M)$ and $\nu_{as}(M–O_c–M)$, (M=W, V) in the region

Fig. 1 Scheme of POM-ILs synthesis procedure.

Fig. 3 FT-IR spectra of $H_5[PW_{10}V_2O_{40}]$ (a), fresh $[TEAPS]_5PW_{10}V_2O_{40}$ (b) and recycled $[TEAPS]_5PW_{10}V_2O_{40}$ (c).

decomposition. At the same time they maintained structure of sulfonic-functionalized triethylamine cation when TEAPS was added. This further proved the heteropoly acid and TEAPS were successfully assembled. Compared with the fresh catalyst, the infrared spectrum of the recycled catalyst was almost unchanged, indicating that Keggin-type structure of the catalyst remained stable after catalytic reaction.

The UV absorption spectrum of these compounds are shown in Fig. 4. As shown Fig. 4, we can find that the absorption bands of $[TEAPS]_5PW_{10}V_2O_{40}$, fresh $[TEAPS]_5PW_{10}V_2O_{40}$ and recycled $[TEAPS]_5PW_{10}V_2O_{40}$ appeared at about 191 nm and 252 nm. The absorption bands were attributed to the charge transfer between oxygen and coordinate metal.[30,34] This can further provide an evidence that Keggin-type structure was still present in fresh $[TEAPS]_5PW_{10}V_2O_{40}$ and recycled $[TEAPS]_5PW_{10}V_2O_{40}$.

3.3 XRD analysis

The phase and structure of the heteropoly compounds were further identified, as shown in Fig. 5. It is clear that the XRD pattern of $[TEAPS]_5PW_{10}V_2O_{40}$ was distinctly different from that of the pure heteropoly acid. For $H_5[PW_{10}V_2O_{40}]$, there were typical and strong diffraction peaks in the range of $2\theta = 7–12°$, $18–24°$, $24–36°$, which revealed its crystalline state. The strong diffraction peaks at $7–12°$ can be considered as the POM anion structure, they were also observed in the XRD pattern of $[TEAPS]_5PW_{10}V_2O_{40}$ in the small angle area, suggesting that the POM anion structure existed in the hybrid material.[30,34] However, $[TEAPS]_5PW_{10}V_2O_{40}$ exhibited a broad diffraction peak in the range of $2\theta = 12–40°$, which revealed its amorphous state, which was consistent with the gel-type phase at room temperature. It is reported that an organized layer-type structure existed in this series of compounds, and the weak connections of the layers leaded to the appearance of smectic gel-type phase.[30,34]

3.4 TG-DSC analysis

TG-DSC curves of typical samples, $H_5PW_{10}V_2O_{40}$ and $[TEAPS]_5$-$PW_{10}V_2O_{40}$, were shown in Fig. 6, which displayed three steps

Fig. 2 ^{1}H NMR (a), ^{13}C NMR (b) and ^{31}P MAS NMR spectra of $[TEAPS]_5PW_{10}V_2O_{40}$.

between 700 and 1100 cm^{-1}. Those four well-known characteristic bands proved the presence of Keggin-type heteropoly anion.[34,35]

Compared with pure heteropolyacids, the M–O_d and P–O_a vibration frequencies of POM-ILs were decreased when sulfo-group grafted ammonium ions were added to POM. This phenomenon could be explained that the electrostatic between the organic cation and heteropolyacid anions were weakened as the anion–anion distance increases.[34] Furthermore, some other characteristic peaks at 1160 cm^{-1}, 2977 cm^{-1} were assigned to $\nu_{S=O}$ and ν_{C-H}, respectively.[34] Since the characteristic peaks still existed, we can infer that these compounds still retained Keggin-type structure of heteropolyanion without

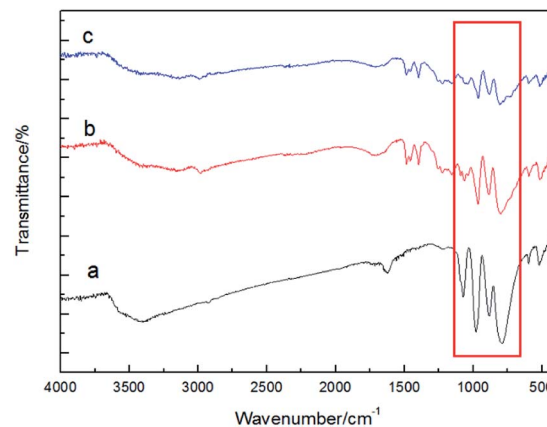**Table 1** The IR spectrum of compounds at 1100–700 cm^{-1}

Vibrations/cm^{-1}	$PW_{10}V_2$	Fresh $[TEAPS]_5PW_{10}V_2O_{40}$	Recycled $[TEAPS]_5PW_{10}V_2O_{40}$
P–O$_a$ stretching	1074	1066	1064
M=O$_d$ stretching	975	968	964
M–O$_b$–M stretching	883	888	890
M–O$_c$–M stretching	794	804	800
S=O bending	—	1160	1158
–CH$_2$ stretching	—	2977	2981
–CH$_2$ scissoring	—	1486	1489
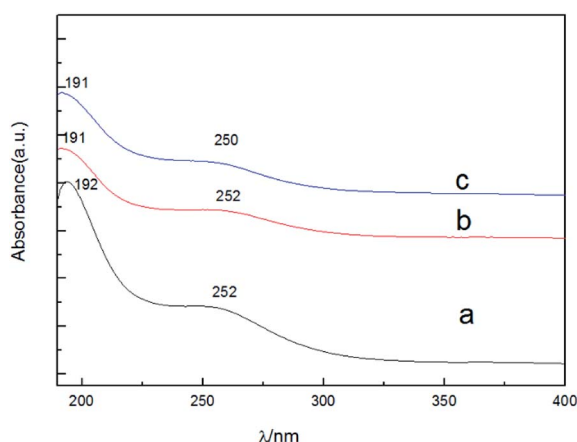
Fig. 4 UV spectra of $H_5[PW_{10}V_2O_{40}]$ (a), fresh $[TEAPS]_5PW_{10}V_2O_{40}$ (b) and recycled $[TEAPS]_5PW_{10}V_2O_{40}$ (c).
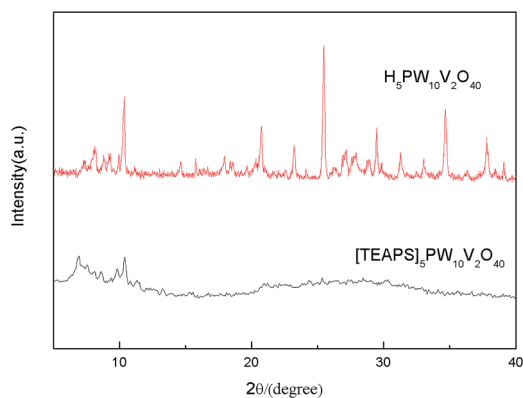
Fig. 5 XRD patterns of $H_5PW_{10}V_2O_{40}$ and $[TEAPS]_5PW_{10}V_2O_{40}$.

Fig. 6 TG-DSC plots of $H_5PW_{10}V_2O_{40}$ (a) and $[TEAPS]_5PW_{10}V_2O_{40}$ (b).

3.5 Determination of acidity of POM-ILs catalysts

Esterification is a typical acid-catalyzed reaction and so it is necessary to measure the acidity of catalysts. The acidity of POM-ILs were determined by potentiometric titration with *n*-butylamine. Potentiometric titration curves of different POM-ILs were shown in Fig. 7. The initial electrode potential (E_i) or pH before the titration demonstrates the maximum strength of the acid sites. At the end of titration, the value from which the plateau is reached (mmol amine per g catalyst) indicates the total number of acid sites.[36,37] The acid strength of heteropoly acid can be judged by initial titration potential (E_i). It is defined as very strong acid ($E_i > 100$ mV), strong acid (0 mV $< E_i < 100$ mV), and weak acid (-100 mV $< E_i < 0$ mV).[37] As shown in Fig. 7, the initial E_i value of all POM-ILs catalysts, $[TEAPS]_4PW_{11}VO_{40} = 341$ mV (pH = 1.25), $[TEAPS]_5PW_{10}V_2O_{40} = 263$ mV (pH = 2.56), $[TEAPS]_6PW_9V_3O_{40} = 229$ mV (pH = 3.13), which meant that acid strength of POM-ILs catalysts are very strong acid. The

weight loss for the $H_5PW_{10}V_2O_{40}$ at 144.7 °C, 220–400 °C and 400–550 °C. The weight loss below 400 °C corresponded to loss of surface adsorption water and protonated water. The primary weight loss between 400–550 °C corresponded to the loss of structure water and decomposition of Keggin-type structure. For $[TEAPS]_5PW_{10}V_2O_{40}$, there was an obvious endothermic peak at 105.4 °C, which corresponded to its melting point. The large weight loss beginning at 350 °C was due to the decomposition of organic cation, suggesting that $[TEAPS]_5PW_{10}V_2O_{40}$ was stable below 350 °C.[30]
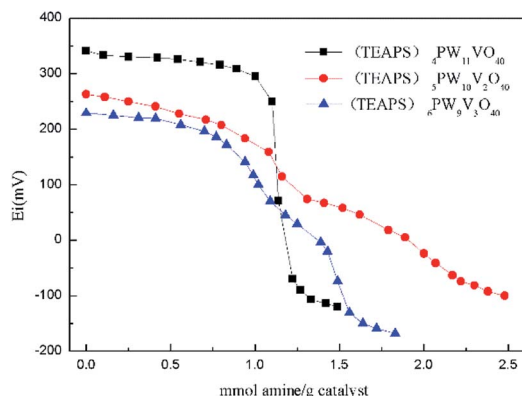
Fig. 7 Potentiometric titration curves of different POM-ILs.

order of acid strength was as follows: $[TEAPS]_4PW_{11}VO_{40}$ > $[TEAPS]_5PW_{10}V_2O_{40}$ > $[TEAPS]_6PW_9V_3O_{40}$, whose order is in accordance with their initial pH values. The number of acid sites was in the following order: $[TEAPS]_5PW_{10}V_2O_{40}$ > $[TEAPS]_4PW_{11}VO_{40}$ > $[TEAPS]_6PW_9V_3O_{40}$.

3.6   Analysis of catalytic esterification reaction process

Conventional homogenous catalyst for esterification is difficult to be separated and reused from product. However, $[TEAPS]_5$-$PW_{10}V_2O_{40}$ catalyst can easily overcome the above-mentioned problems due to a characteristic of temperature-controlled liquid–solid separation. Its reaction process with temperature change was shown in Fig. 8. At the beginning of the reaction, the catalyst was undissolved in the reactant mixture and formed a heterogeneous system (Fig. 8a). At reaction temperature, the catalyst was dissolved in the mixture, the system transferred from heterogeneous to homogeneous and became yellow owing to the colour of catalyst itself (Fig. 8b). At the end of the reaction, with temperature decreased, the produced colourless ester was in the upper level of the resulting mixture, and the catalyst gradually precipitated at bottom (Fig. 8c). Therefore the catalyst could be easily recycled from the products by simple filtration.

Table 2 listed the results of esterification reaction over various catalysts. The esterification of chloroacetic acid with *n*-pentyl alcohol system can be self-catalytic and reach only 75% of esterification rate because of its strong acidity (entry 1). The
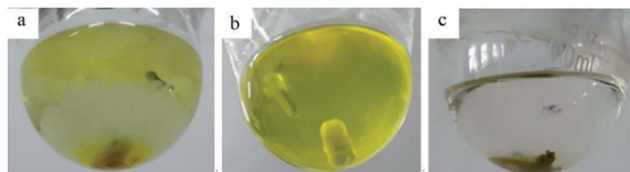

Fig. 8 Photographs of the esterification of chloroacetic acid and *n*-pentyl alcohol over $[TEAPS]_5PW_{10}V_2O_{40}$ catalyst. (a) $[TEAPS]_5PW_{10}V_2$-O_{40} (light yellow solid at bottom), chloroacetic acid (white solid in the middle), and *n*-pentyl alcohol (liquid in the upper level) before reaction; (b) homogeneous yellow mixture during the reaction; (c) the catalyst has precipitated at bottom, the colourless product is in the upper level at the end of the reaction.

catalytic activity of conventional catalyst, such as sulfuric acid, presented unsatisfactory esterification rate of 87.47% (entry 2). Although serial heteropolyacid catalysts exhibited high esterification rate (nearly 95%, entry 3–5), it is hardly separated from the product.[36] However, it is noted that POM-ILs catalysts not only could be separated from the product conveniently but also exhibited notable catalytic activity (95.3–98.75%, entry 6–8).

Esterification reaction mechanism of chloroacetic acid using $[TEAPS]_5PW_{10}V_2O_{40}$ catalyst was proposed in Fig. 9. Carbonyl of chloroacetic acid was protonated by hydrogen ions which were provided by functional group TEAPS in the ionic liquid catalysts and *n*-pentyl alcohol attack carbocation of carbonyl in chloroacetic acid. The ester was generated by dehydrate process.

We measured the acidity of POM-ILs by potentiometric titration with *n*-butylamine to analyze any relationship between acidic properties and catalytic activity. As previous mentioned, the order of acid strength was as follows: $[TEAPS]_4PW_{11}VO_{40}$ > $[TEAPS]_5PW_{10}V_2O_{40}$ > $[TEAPS]_6PW_9V_3O_{40}$. The number of acid sites was in the following order: $[TEAPS]_5PW_{10}V_2O_{40}$ > $[TEAPS]_4PW_{11}VO_{40}$ > $[TEAPS]_6PW_9V_3O_{40}$.

As esterification reaction is a typical acid-catalyzed mechanism, generally, the higher acid strength of catalysts, the higher catalytic activities. However, the esterification rate of $[TEAPS]_4PW_{11}VO_{40}$ was less than $[TEAPS]_5PW_{10}V_2O_{40}$ or $[TEAPS]_6PW_9V_3O_{40}$. This result could be attributed to their different melting point and solubility in reaction system. $[TEAPS]_4PW_{11}VO_{40}$ catalyst has higher melting point (145.0 °C) and partly dissolved in the reactants at reaction temperature, and that it was more likely to result in lower activity. Another reason may be resulted from its less number of acid sites. From the result of esterification reaction over various catalysts and their phenomenon, it is assumed that the sulfonic-functionalized triethylamine cation provides the acid site responsible for the high activity in esterification, and the static interaction between organic cation and polyoxometalate anion is crucial to temperature responsive characteristics, which is responsible for the solid–liquid–solid phase transformation and catalyst separation.

The effect of various reaction parameters, including the amount of catalyst, water carrier volume, reaction temperature, the ratio of alcohol to acid, were investigated by an orthogonal experiment method using $(TEAPS)_5PW_{10}V_2O_{40}$ as catalyst. The above-mentioned four reaction parameters and three orthogonal levels were reasonably designed using $L9(3^4)$ orthogonal table. The effect of every experiment factor and level on esterification rate was shown in Table 3. Range analysis showed that the reaction temperature was the dominant factor, next were water carrier volume, the amount of catalyst and the ratio of alcohol to acid in descending order. The optimized solution was that the amount of catalyst was 0.2 g, water carrier was 10 mL, reaction temperature was 140 °C, and the ratio of alcohol to acid was 1.2 : 1.

3.7   Reusability of $[TEAPS]_5PW_{10}V_2O_{40}$ catalyst

As the catalyst could be easily recovered by simple filtration at the end of the reaction, the catalyst without any regeneration

Table 2 Results of esterification reaction over various catalysts[a]

Entry	Catalyst	Phenomenon	Esterification rate (%)
1	Without catalyst	Homogenous[1,2]	75.00
2	H_2SO_4	Homogenous[1,2]	87.47
3	$H_4PW_{11}VO_{40}$	Homogenous[1,2]	94.52
4	$H_5PW_{10}V_2O_{40}$	Homogenous[1,2]	94.63
5	$H_6PW_9V_3O_{40}$	Homogenous[1,2]	95.00
6	$[TEAPS]_4PW_{11}VO_{40}$	Partly dissolved[1], phase seperation[2]	95.30
7	$[TEAPS]_5PW_{10}V_2O_{40}$	Homogenous[1], phase separation[2]	98.75
8	$[TEAPS]_6PW_9V_3O_{40}$	Homogenous[1], phase separation[2]	97.54

[a] 1, 2 represent the catalyst state during reaction and after reaction, respectively.
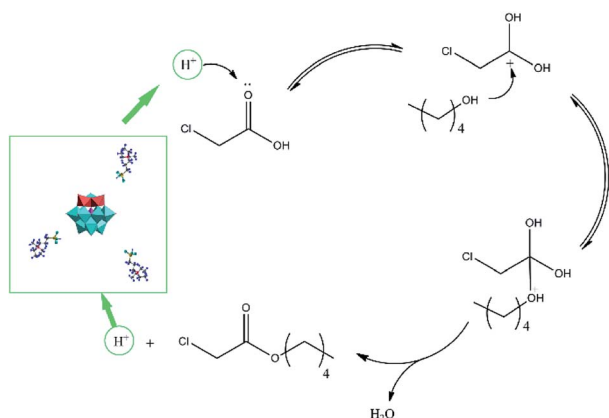

Fig. 9 Esterification reaction mechanism of chloroacetic acid using $[TEAPS]_5PW_{10}V_2O_{40}$ catalyst.

Table 3 Orthogonal experimental scheme and results of chloroacetates catalyzed by $(TEAPS)_5PW_{10}V_2O_{40}$[a]

No.	A (g)	B (mL)	C (°C)	D	Esterification rate (%)
1	1(0.1)	1(5)	1(100)	1(1.1)	80.21
2	1(0.1)	2(10)	2(120)	2(1.2)	91.82
3	1(0.1)	3(15)	3(140)	3(1.3)	94.26
4	2(0.2)	1(5)	2(120)	3(1.3)	89.09
5	2(0.2)	2(10)	3(140)	1(1.1)	97.78
6	2(0.2)	3(15)	1(100)	2(1.2)	85.56
7	3(0.3)	1(5)	3(140)	2(1.2)	93.14
8	3(0.3)	2(10)	1(100)	3(1.3)	84.26
9	3(0.3)	3(15)	2(120)	1(1.1)	87.03
K_1	266.29	262.44	250.03	265.02	
K_2	272.43	273.86	267.94	270.52	
K_3	264.43	266.85	285.18	267.61	
R	8.00	11.42	35.15	5.5	

Factor order: $C > B > A > D$
Optimal solution: $A_2B_2C_3D_2$

[a] A, B, C, D represent the amount of catalyst, water carrier volume, reaction temperature, the ratio of alcohol to acid, respectively. The numbers in brackets represent orthogonal level order, K_1, K_2, K_3 represent the sum of the experimental results at each level, respectively. R represents range.
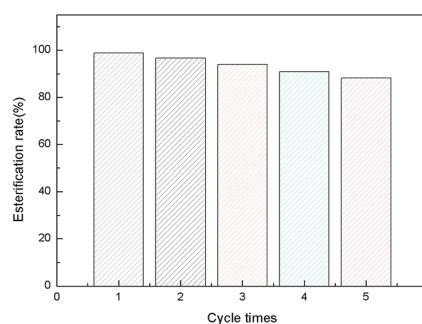

Fig. 10 Reusability of $[TEAPS]_5PW_{10}V_2O_{40}$ catalyst on the esterification reaction.

was reused for the next run. The reusability of $[TEAPS]_5PW_{10}V_2O_{40}$ in the esterification reaction system was shown in the Fig. 10. The esterification rate decreased from 98.75% for the first run to 90.97% for the fifth run. The IR and UV spectra for the recycled catalyst was well consistent with the fresh catalyst (see Fig. 3 and 4), which meant that structure of the catalyst was stable. Thus, the slight decrease in catalytic activity result from the slight loss of catalyst during dissolution process.

4. Conclusions

A series of thermo-regulated ionic liquids catalysts were synthesized by ionic self-assembly method with sulfonic-functionalized triethylamine cation and vanadium-substituted heteropolyacids. The ionic liquid, $[TEAPS]_5PW_{10}V_2O_{40}$ exhibited the highest catalytic activity with esterification rate of 98.75% under the optimized conditions. The sulfonic-functionalized triethylamine cation provided the acid site responsible for the high activity in esterification, and the static interaction between organic cation and polyoxometalate anion led to temperature responsive characteristics, which was responsible for the solid–liquid–solid phase transformation and separation. The catalyst could be easily recycled by simple filtration and reused without significant decrease.

Conflicts of interest

There are no conflicts to declare.

Acknowledgements

Notes and references

1 G. D. Yadav and M. B. Thathagar, *React. Funct. Polym.*, 2002, **52**, 99–110.

2 I. V. Kozhevnikov, *Chem. Rev.*, 1998, **98**, 171–198.

3 A. Alsalme, E. F. Kozhevnikova and I. V. Kozhevnikov, *Appl. Catal., A*, 2010, **390**, 219–224.

4 A. Démolis, N. Essayem and F. Rataboul, *ACS Sustainable Chem. Eng.*, 2014, **2**, 1338–1352.

5 P. Mäki-Arvela, T. Salmi, M. Sundell, K. Ekman, R. Peltonen and J. Lehtonen, *Appl. Catal., A*, 1999, **184**, 25–32.

6 A. Morone, M. Apte and R. A. Pandey, *Renewable Sustainable Energy Rev.*, 2015, **51**, 548–565.

7 Z. R. Xie, H. Wu, Q. Y. Wu and L. M. Ai, *RSC Adv.*, 2018, **8**, 13984–13988.

8 M. Li, D. Y. Chen and X. F. Zhu, *Chin. J. Catal.*, 2013, **34**, 1674–1682.

9 X. T. Hu, Z. Zhou, D. F. Sun, Y. T. Wang and Z. B. Zhang, *Catal. Lett.*, 2009, **133**, 90–96.

10 E. Rafiee and S. Eavani, *J. Mol. Liq.*, 2014, **199**, 96–101.

11 T. Ooi and K. Maruoka, *Angew. Chem.*, 2007, **119**, 4300–4345.

12 G. A. N. Anwar, F. Laffir, C. Dickinson, M. Vagin and T. Mccormac, *Electrochim. Acta*, 2018, **265**, 254–258.

13 Y. Y. Li, X. F. Wu, Q. Y. Wu, H. Ding and W. F. Yan, *Ind. Eng. Chem. Res.*, 2014, **53**, 12920–12926.

14 A. B. Bourlinos, K. Raman, R. Herrera, Q. Zhang, L. A. Archer and E. P. Giannelis, *J. Am. Chem. Soc.*, 2004, **126**, 15358–15359.

15 C. N. Dai, J. Zhang, C. P. Huang and Z. G. Lei, *Chem. Rev.*, 2017, **117**, 6929–6983.

16 R. L. Vekariya, *J. Mol. Liq.*, 2017, **227**, 44–60.

17 A. C. Cole, J. L. Jensen, I. Ntai, K. L. T. Tran, K. J. Weaver, D. C. Forbes and J. H. Davis, *J. Am. Chem. Soc.*, 2002, **124**, 5962–5963.

18 C. X. Xie, H. L. Li, L. Li, S. T. Yu and F. S. Liu, *J. Hazard. Mater.*, 2008, **151**, 847–850.

19 M. Bonamico, A. Medici, C. Chiesa and F. Carpino, *Green Chem.*, 2012, **14**, 1736–1742.

20 A. L. Zhu, M. Y. Wang, L. J. Li and J. J. Wang, *RSC Adv.*, 2015, **5**, 73974–73979.

21 Y. Leng, J. Wang, D. R. Zhu, X. R. Ren, H. Q. Ge and L. Shen, *Angew. Chem., Int. Ed.*, 2009, **48**, 168–171.

22 J. J. Chen, J. C. Ye, X. G. Zhang, M. D. Symes, S. C. Fan, D. L. Long, M. S. Zheng, D. Y. Wu, L. Cronin and Q. F. Dong, *Adv. Energy Mater.*, 2018, **8**, 1701021.

23 J. Azizullah, M. Al-Rashida, A. Haider, U. Kortz, S. A. Joshi and J. Iqbal, *ChemistrySelect*, 2018, **3**, 1472–1479.

24 Z. Chen, W. B. Bu, D. L. Ni, C. J. Zuo, C. Chao, Q. Li, L. L. Zhang, Z. Wang and J. L. Shi, *J. Am. Chem. Soc.*, 2016, **138**, 8156–8164.

25 T. P. Huang, Z. R. Xie, Q. Y. Wu and W. F. Yan, *Dalton Trans.*, 2016, 3958–3963.

26 Z. R. Xie, Q. Y. Wu, W. S. Dai and F. W. He, *Int. J. Electrochem. Sci.*, 2018, **13**, 11684–11690.

27 Z. R. Xie, Q. Y. Wu and L. M. Ai, *Funct. Mater. Lett.*, 2018, **11**, 1850059.

28 L. M. Ai, Z. Q. Wang, F. W. He and Q. Y. Wu, *RSC Adv.*, 2018, **8**, 34116–34120.

29 X. Tong, N. Q. Tian, W. M. Zhu, Q. Y. Wu, F. H. Cao and W. F. Yan, *J. Alloys Compd.*, 2012, **544**, 37–41.

30 X. F. Wu, W. Wu, Q. Y. Wu and W. F. Yan, *Langmuir*, 2017, **33**, 4242–4249.

31 (*a*) X. Tong, N. Q. Tian, W. Wu, W. M. Zhu, Q. Y. Wu, F. H. Cao, W. F. Yan and A. B. Yaroslavtsev, *J. Phys. Chem. C*, 2013, **117**, 3258–3263; (*b*) Q. Y. Wu, X. Tong and X. F. Wu, *J. Xuzhou Inst. Technol., Nat. Sci. Ed.*, 2011, **26**, 1–8.

32 (*a*) X. F. Wu, Ph. D. thesis, Zhejiang University, China, 2017; (*b*) X. F. Wu, Y. Y. Li, Q. Y. Wu, H. Ding and W. F. Yan, *Phys. Chem. Chem. Phys.*, 2014, **16**, 24598–24603.

33 I. V. Kozhevnikov, K. R. Kloetstra, A. Sinnema, H. W. Zandbergen and H. V. Bekkum, *J. Mol. Catal. A: Chem.*, 1996, **114**, 287–298.

34 X. F. Wu, T. P. Huang, X. Tong, Z. R. Xie, W. X. Chen, Q. Y. Wu and W. F. Yan, *RSC Adv.*, 2015, **5**, 21973–21977.

35 X. F. Wu, X. Tong, Q. Y. Wu, H. Ding and W. F. Yan, *J. Mater. Chem. A*, 2014, **2**, 5780–5784.

36 E. Rafiee and F. Mirnezami, *J. Mol. Struct.*, 2017, **1130**, 296–322.

37 E. Rafiee, M. Joshaghani, S. Eavani and S. Rashidzadeh, *Green Chem.*, 2008, **10**, 982–989.